

Feature Selection

Generative AI Academy

Part 4: Neural Networks — Relevance Aggregation

Bruno lochins Grisci
bigrisci@inf.ufrgs.br

Institute of Informatics
Federal University of Rio Grande do Sul

May 20, 2025

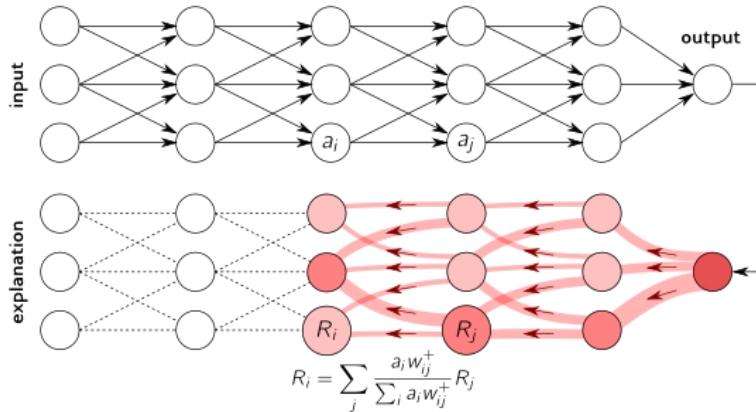
Outline

- 1 Introduction
- 2 Relevance Aggregation
- 3 Weighted t-SNE
- 4 Application to cancer data
- 5 Conclusion

Objectives

- Deep learning interpretability in tabular data
- Visualization of feature scoring
- Knowledge discovery from biological data

Layer-wise relevance propagation



[Bach et al., 2015]

Relevance propagation rules

$$R_j = \sum_k \left(\alpha \frac{a_j w_{jk}^+}{\sum_j a_j w_{jk}^+} - \beta \frac{a_j w_{jk}^-}{\sum_j a_j w_{jk}^-} \right) R_k \quad (1)$$

$$R_j = \sum_k \frac{w_{jk}^2}{\sum_j w_{jk}^2} R_k \quad (2)$$

[Montavon et al., 2018]

LRP example

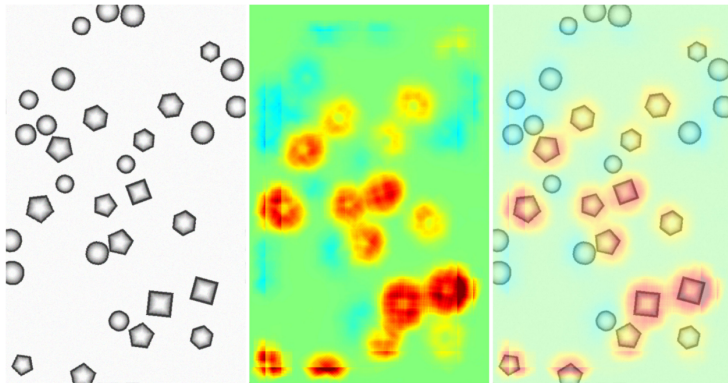


Fig 6. Pixel-wise decomposition for Bag of Words features over χ^2 -kernels using the Taylor-type decomposition for the third layer and the layer-wise relevance propagation for the subsequent layers. Left: The original image. Middle: Pixel-wise prediction. Right: Superposition of the original image and the pixel-wise prediction. The decompositions were computed on tiles of size 102×102 and having a regular offset of 34 pixels. The decompositions from the overlapping tiles were averaged. In the heatmap, based on linearly mapping the interval $[-1, +1]$ to the jet color map available in many visualization packages, green corresponds to scores close to zero, yellow and red to positive scores and blue color to negative scores. See text for interpretation.

[Bach et al., 2015]

Applications

- ① MRI-Based Alzheimer's disease classification [Böhle et al., 2019]**
- ② Prediction of morphological and molecular tumor profiles [Binder et al., 2018]**
- ③ Therapy predictions of metastatic breast cancer [Yang et al., 2018]**

Outline

1 Introduction

2 Relevance Aggregation

3 Weighted t-SNE

4 Application to cancer data

5 Conclusion

The face of the data

	A	B	C	D	E	F	G	H	I	J	K	L
1	samples	type	1007_s_at	1053_at	117_at	121_at	1255_q_at	1294_at	1316_at	1320_at	1405_i_at	1431_at
2	GSM362958 CEL_g	HCC	6.80119760710874	4.55318894640395	4.78779002909496	5.43089267353575	3.25022189170724	6.27268846989046	3.413404746412	3.37490984706688	3.65411613599682	3.80498352183284
3	GSM362959 CEL_g	HCC	7.5859561626449	4.1935401301431	3.76318259460317	6.00359349944804	3.3093876781399	6.29192656845271	3.75477701364209	3.586760253072689	5.13715938611725	8.6224754628958
4	GSM362960 CEL_g	HCC	7.8033704813439	4.134075383015	3.4331130356077	5.3905709653068	3.47694393405601	5.82571255203611	3.5050359852534	3.68733289144417	4.51517535182232	12.681391099332
5	GSM362964 CEL_g	HCC	6.92082674034097	5.00953034120241	5.64529670292514	3.38750347840899	6.47045799349579	3.62924920818033	3.57753407054759	5.19262423621283	11.7594120751621	
6	GSM362965 CEL_g	HCC	5.55648015323744	4.5990104902905	4.0661551575957	6.34453626250212	3.37208126560519	5.4392803435272	3.76221336675644	3.44071407349146	4.96162490905675	10.318552481299
7	GSM362966 CEL_g	HCC	7.30668391006144	4.36869795997217	3.72489358089459	5.61296709029724	3.22458864145194	6.11220891725254	3.466610514513963	3.31495102218217	4.07110192135605	11.944573918641
8	GSM362970 CEL_g	HCC	6.5129285592314	6.44654460565343	3.87271884659331	5.6865917726611	3.30420310641847	6.44245508624605	3.37885664430557	3.26577268196747	4.64010462565657	10.196788009446
9	GSM362971 CEL_g	HCC	6.82697854213955	4.01936601587141	4.12079159820386	5.71730950146647	3.21870382202531	6.60032703329945	3.77286897801043	3.5134618215437	5.8883125325068	12.5153547104115
10	GSM362972 CEL_g	HCC	5.8207882784831	4.1594009925679	3.72900435654028	6.2171154325368	1.81883144008311	1.13059119281839	3.67742123833104	3.401679707956	4.7839199002284	12.6981102815037
11	GSM362976 CEL_g	HCC	9.5275328805125	3.90591379539624	5.90492176466688	3.95482009554468	3.367744999844	3.367744999844	3.52332059455147	5.477884729050527	5.60507448655527	
12	GSM362977 CEL_g	HCC	5.628561513269	3.928199595004	4.8570130130183	6.30642665784121	3.796187341023	5.04674289874766	3.66233421553639	3.57668134999204	4.22799212949975	3.74834598474946
13	GSM362978 CEL_g	HCC	6.09641757361098	2.9820337003072	3.99306026148466	5.46529670292514	3.36260682793352	6.7909176114277	3.4741827281083	3.05664240505734	4.20849010621795	4.29009126149721
14	GSM362982 CEL_g	HCC	3.3876265707729	4.687953867814	3.8547825155535	6.21822737707656	3.08223207212912	5.23572609261187	3.552173049093	3.46640332016121	3.7637937825426	7.1445567739736
15	GSM362984 CEL_g	HCC	3.6752538336142	4.04805125867143	3.67049139915035	5.9883735425255	3.20466525828664	6.44163286878761	3.45277713125766	3.4725149425959	11.1891452383344	
16	GSM362986 CEL_g	HCC	6.93260469946496	2.692912419209	4.2163355125976	5.58171993888985	3.0218545778632	6.0291244026108	3.35290934154539	3.34277749465531	12.7316517113786	
17	GSM362988 CEL_g	HCC	7.2553584490416	4.6356302990791	4.23650457584559	5.29924917415942	3.2199078785232	6.2219044941213	3.5584663783093	3.6404054681158	12.7975986371997	11.7634073359866
18	GSM362992 CEL_g	HCC	1.66996096217955	4.29595093006300	3.44251451271291	0.57607607238335	3.22929063619527	6.96633907500718	6.367405708742898	3.580203711920004	4.32285734565323	8.2690145449646
19	GSM362993 CEL_g	HCC	8.702615185967	4.5725798417081	6.303293491651	5.6130239415618	3.15232780241425	6.2777278935936	3.583634026302103	3.503647423723948	8.423115240843	16.859041300882
20	GSM362994 CEL_g	HCC	6.76482136993378	3.8847215302088	3.88472119278071	6.0072031310914	3.1903774940686	4.089177801707	3.4618252773527	3.51771948115732	3.54822654670111	12.5643275309247
21	GSM363008 CEL_g	HCC	6.8917326997187	3.899348301462301	4.1541839307624	5.3760682793352	4.593989956914494	5.359989956914494	5.36780910067754	6.74269327834105	11.3200047886433	
22	GSM363009 CEL_g	HCC	9.245154515011505	5.52516416423998	4.242973789939	5.3214200126194	4.19532173601215494	5.75161730617912	5.022332854056	4.9442157521817	4.62115010902122	16.04134987458
23	GSM363010 CEL_g	HCC	10.2036980958542	4.38759374226001	4.86040327547265	4.04716475232973	3.2273815195483	4.88405445575257	4.376517419435043	5.1693521312444	11.661380418393	
24	GSM363011 CEL_g	HCC	6.78216616252534	4.937940090817	3.6565506589873	5.372890974041238	6.20957947404100	4.371624344426	3.7648080512345	3.81215365677371	8.2870253684081	
25	GSM363012 CEL_g	HCC	0.1509327818864	4.94432521740907	4.27735642569507	6.557654047340037	3.1589373372076	5.8895538934893	6.71036456283506	3.26732206180902	12.609205710782	
26	GSM363013 CEL_g	HCC	7.480112253337	4.3995457528765	4.2094751858132	5.16120063448354	3.20182366910594	6.22815259526864	3.67104645628354	3.25287599281981	5.53077999103044	7.38172245534906
27	GSM363015 CEL_g	HCC	7.7372315574563	5.6189397311947	4.8725015728996	5.05182038028231	3.0217091890907	5.1170954383187	4.7179170998197	3.62029158436817	3.96904725028263	13.317213253045325
28	GSM363016 CEL_g	HCC	5.86680991526679	4.24469962256086	3.86169690511572	5.833417211962545	3.4784445443504	3.66668991339404	3.427561976734	3.9230334246936	5.531686724325	
29	GSM363017 CEL_g	HCC	2.68894922992686	5.30140674043119	4.10753935865564	5.6544839671474552	3.08014868963274	6.5002552426958	3.92602919511267	3.4649327522747	4.10679173344	10.539449705933
30	GSM363029 CEL_g	HCC	6.84321505000151	4.5458289885644	3.59398834138624	4.940666220427	1.11064895778759	4.6083940340904	5.30998834080277	5.7360227756437	10.458677390233	
31	GSM363030 CEL_g	HCC	8.6863899770449	4.9166066842904	4.1022107051008	4.9822808760507	3.05775121546522	5.68917840090946	3.4036776980946	3.3004194003122	3.62365168020831	9.97750595522057
32	GSM363031 CEL_g	HCC	5.736641163640904	4.3292110700053	3.996989825744993	4.9265667526748	4.15452774727111	3.6203203797995	3.904336165153503	3.53895027957314	4.7083544108223	10.065292712843
33	GSM363032 CEL_g	HCC	6.681193094872018	3.659073128996	3.8776228480877	5.548796265681	3.1296312034136	4.433717645219667	3.77207141948621	3.67379686009843	11.8902326658131	
34	GSM363033 CEL_g	HCC	6.60768163026333	4.171716477843	3.848107658051	5.01628590431952	3.157076745228669	3.64215649550671	3.674943032626603	3.49381996037004	5.76793633699196	6.5217075209241
35	GSM363034 CEL_g	HCC	9.67964791042211	5.37545207119183	5.7694986644884	5.35963701535011	3.253787012340821	3.6421264955036	3.73654202462175	12.2657446353535		
36	GSM363035 CEL_g	HCC	6.62275948748058	3.86720135022073	3.92974198620237	5.8117343745424161	3.2779701968842	4.2004136620377	3.8178044397589	3.54364896214802	4.861699656137	11.9277673380745
37	GSM363036 CEL_g	HCC	6.03010301049745	4.84806590505357	4.0722834473597	3.50422998139408	3.2739363373742	5.715589785342464	3.81279876757055	3.307948360305709	3.13495976558155	12.3562967481996
38	GSM363037 CEL_g	HCC	5.96883400299292	5.07709282114	4.016747722127	5.11529423091779	3.26608779039104	5.33686576043233	3.59967637430373	3.292695334222	12.18974115421	
39	GSM363038 CEL_g	HCC	6.26981138983515	5.654278111044	3.3963685248947	5.4906027933608	3.1095369585928	5.57152658959456	5.3194553635121	3.62365168020831	4.6227119271966	
40	GSM363039 CEL_g	HCC	6.61577396325334	4.1807100052337	3.76709381308107	3.796545405074	3.17654464505074	3.6188456950568	3.7101801424204	3.7414830860491	3.5446217638714	13.3424681294999
41	GSM363048 CEL_g	HCC	3.20267233754949	4.6213477958137	3.8344276947656	5.1522916302533	2.9591036801951	5.70770318717344	3.296032665558	3.567484762392217	3.7063827601181	8.8825327401174
42	GSM363049 CEL_g	HCC	6.25295225258582	4.1786572153331	3.65382324244556	3.615033996351523	3.05976531101919	1.886786303346	3.61614628150378	3.55644729092067	3.77363617472517	12.6841590415012
43	GSM363053 CEL_g	HCC	5.965017490211	5.37545207119183	5.7694986644884	5.4485163190364	3.18768453730564	5.85154392697053	5.363761505162	5.2949946161624	4.4065500350959	
44	GSM363055 CEL_g	HCC	9.67749449446444	4.236620301723233	5.23605763577932	4.24635051652083	1.530517591611565	2.32843289811646	5.2949946161624	5.363761505162	5.2949946161624	4.4065500350959
45	GSM363056 CEL_g	HCC	8.14583616094427	5.58254840036409	4.2445277509092	5.39676018627489	3.06267439900211	5.85566084570108	3.67273814063241	3.54230718136662	3.54475606512553	3.3842863831052
46	GSM363057 CEL_g	HCC	6.17618317374308	3.87083017023233	7.235386078907206	5.1933205282025	3.0825243110478	5.1542025140122	3.40253690512998	3.67548330010597	3.3924772095767	11.810131820272

Motivation I

- ① Heterogeneity present in the data makes interpretation at the sample level less informative or clear.
- ② Loss of selectivity in LRP when applied to fully connected layers.
- ③ Fixed order of tabular data features.
- ④ Takes all features at once.
- ⑤ Interaction between different features.
- ⑥ Does not necessarily discard redundant features.
- ⑦ No iterative selection.
- ⑧ No need to retrain models or create local surrogates to approximate the behavior of the black-box predictor.

Motivation II

Table: The difference between seeing the “raw” relevance from LRP and the relevance scores from relevance aggregation.

	240701_at	223259_at	1552801_at	1568691_at	207226_at	217051_s_at	...
s105	0.065	0.062	0.049	0.009	0.003	0.003	...
s101	0.036	0.049	0.016	0.005	0.002	0.008	...
s162	0.043	0.034	0.037	0.030	0.017	0.003	...
s200	0.018	0.014	0.006	0.008	0.002	0.004	...
s183	0.014	0.015	0.008	0.007	0.003	0.001	...
s174	0.024	0.027	0.043	0.026	0.013	-0.001	...
...
score	0.416	0.390	0.278	0.158	0.076	0.030	...

Relevance aggregation

Data: $D_{n \times m}$: data, c : classes, $network$: neural network

Result: Ordered relevance scores

begin

```
R, S, score ← [ ] ;
train network on  $D_{n \times m}$ ;
for sample1 × m in  $D_{n \times m}$  do
    out ← predict(network, sample1 × m);
    rel1 × m ← compute_relevance(network, sample1 × m, out);
    rel1 × m ← abs(rel1 × m) / max(abs(rel1 × m));
    Rsample ← rel1 × m;
end
for featn × 1 in  $R_{n \times m}$  do
    for class in  $c$  do
        | Sfeat, class ← average(featn ∈ class);
    end
end
for feat1 × c in  $S_{m \times c}$  do
    | scorefeat ← average(feat1 × c);
end
return sort(scorem × 1);
end
```

Questions

- ① Do the input features with larger scores convey relevant information about the original data?**
- ② Are they contributing the most to the neural network's output?**

Synthetic data

Table: Synthetic datasets.

	Task	Type	Classes	Features	Relevant	Samples	Source
XOR	Classification	Binary	2	50	2	500	[Tan et al., 2009]
	Regression	Binary	-	50	2	500	[Tan et al., 2009]
syn	Classification	Real	3	1000	5	1000	sklearn make_classification
	Regression	Real	-	100	4	1000	sklearn make_sparse_uncorrelated

XOR truth table

$$0 \oplus 0 = 0$$

$$1 \oplus 0 = 1$$

$$0 \oplus 1 = 1$$

$$1 \oplus 1 = 0$$

Selection: Relevance aggregation

	SCORE	ZERO	ONE
REL002	0,919074	0,922061	0,916088	1	1	1	0	0	0
REL001	0,897107	0,991642	0,802571	1	1	1	1	1	1
IRR003	0,062693	0,022876	0,10251	1	1	1	0	0	0
IRR007	0,046291	0,010313	0,082269	1	1	1	1	1	1
IRR045	0,044367	0,013873	0,074861	1	1	0	0	1	0
...
IRR005	0,004698	0,003099	0,006297	1	1	1	0	1	0

Table heatmap for XOR (classification) dataset.

	SCORE	0	1	2
REL002	0,38	0,36	0,75	0,20	1,20	-0,55	0,11	-0,94	2,33	0,20
RED005	0,27	0,14	0,24	0,57	-1,67	-1,83	-0,76	-1,21	4,01	1,46
REL001	0,26	0,18	0,17	0,55	-2,11	-2,25	-1,61	-1,72	0,19	0,99
REL003	0,22	0,52	0,20	0,11	-1,06	0,74	0,66	1,34	2,11	0,50
RED004	0,07	0,04	0,09	0,09	-0,22	-0,15	-0,25	-0,14	-0,93	-0,08
IRR083	0,03	0,02	0,02	0,05	-0,14	-0,27	-1,86	1,12	-0,84	1,23
...
IRR801	0,02	0,02	0,02	0,03	0,50	-0,89	-0,50	0,86	0,67	-2,03
IRR082	0,01	0,01	0,01	0,00	-0,42	-0,27	0,50	0,65	0,57	-0,43

Table heatmap for synthetic 3-classes dataset.

Figure: Excerpt of the table heatmaps for the XOR (classification) and 3-classes synthetic data.

Selection accuracy

Table: Selection accuracy for the synthetic datasets. This table presents the average “selection accuracy” and standard deviation for four feature selection algorithms on four synthetic datasets. We define the “selection accuracy” as the ratio of the r truly relevant features ranked in the r first positions on the selection of each algorithm.

	XOR (classification)	XOR (regression)	Synthetic 3-classes	Synthetic regression
RelAgg	$1.00 \pm .00$	$1.00 \pm .00$	$1.00 \pm .00$	$0.97 \pm .07$
Decision Tree	$0.35 \pm .39$	$0.00 \pm .00$	$0.78 \pm .06$	$0.75 \pm .00$
mRMR	$0.00 \pm .00$	-	$0.80 \pm .00$	-
Kruskal-Wallis	$0.05 \pm .15$	-	$0.94 \pm .09$	-

Visualization

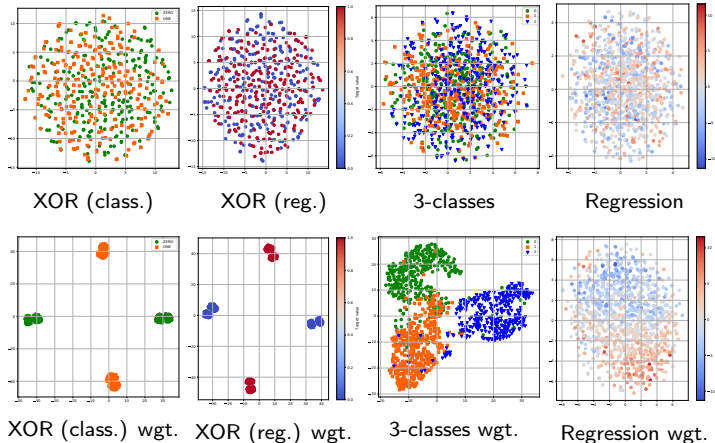


Figure: Visualization of synthetic datasets with t-SNE and weighted t-SNE.

Prediction performance

Table: Classification and regression performance of different algorithms for all datasets. This table presents the average F1 score or MSE and standard deviation from stratified 10-fold cross-validation.

	Classification (F1 score)				Regression (MSE)		
	XOR	3-classes	Breast cancer	E-commerce	XOR	Synthetic	ENEM
NN	0.982 ± .021	0.691 ± .048	0.900 ± .029	0.759 ± .013	0.018 ± .019	3.295 ± .384	8392.814 ± 1186.210
DT	0.499 ± .069	0.829 ± .023	0.599 ± .039	0.793 ± .015	0.266 ± .018	5.423 ± .904	6630.980 ± 268.285
SVM	0.629 ± .000	0.696 ± .000	0.905 ± .000	0.669 ± .000	0.202 ± .000	4.030 ± .000	7563.633 ± .000
SVM (RelAgg)	1.000 ± .000	0.922 ± .000	0.956 ± .019	0.777 ± .001	0.010 ± .000	1.612 ± .327	6354.633 ± 200.827
SVM (DT)	0.653 ± .174	0.916 ± .004	0.843 ± .086	0.763 ± .020	0.325 ± .014	2.429 ± .000	6128.120 ± 79.470
SVM (mRMR)	0.515 ± .005	0.922 ± .001	0.514 ± .023	0.312 ± .126	-	-	-
SVM (KW)	0.513 ± .006	0.922 ± .000	0.812 ± .078	0.780 ± .000	-	-	-

Questions

- ① Do the input features with larger scores convey relevant information about the original data?**
- ② Are they contributing the most to the neural network's output?**

Feature impact

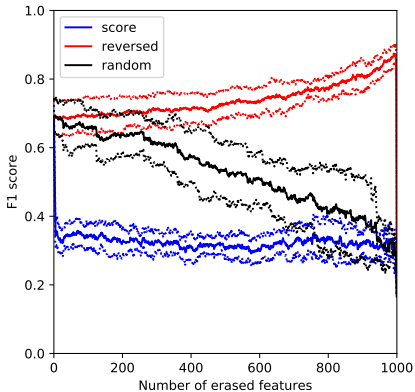


Figure: Perturbation analysis for neural networks trained on the synthetic 3-classes dataset.

Feature impact - Classes

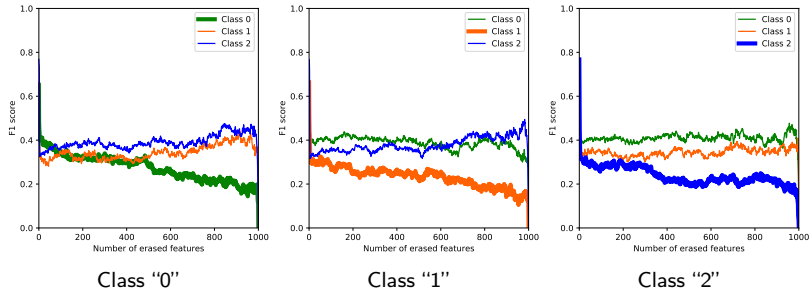


Figure: Perturbation analysis for neural networks trained on the synthetic 3-classes dataset.

Real-world data

Table: Real-world datasets.

	Task	Type	Classes	Features	Samples	Source
Breast cancer	Classification	Real	6	54675	151	[Feltes et al., 2019]
e-commerce	Classification	Mixed	2	67	12330	[Sakar et al., 2019]
ENEM 2016	Regression	Mixed	-	232	13730	MEC - Kaggle

Prediction performance

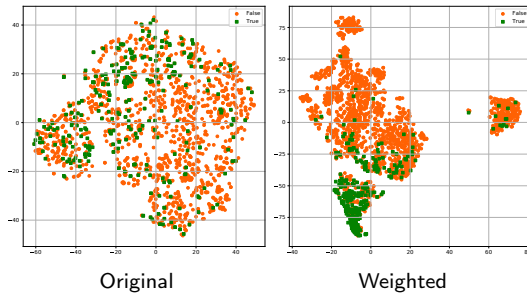
Table: Classification and regression performance of different algorithms for all datasets. This table presents the average F1 score or MSE and standard deviation from stratified 10-fold cross-validation.

	Classification (F1 score)				Regression (MSE)		
	XOR	3-classes	Breast cancer	E-commerce	XOR	Synthetic	ENEM
NN	0.982 ± .021	0.691 ± .048	0.900 ± .029	0.759 ± .013	0.018 ± .019	3.295 ± .384	8392.814 ± 1186.210
DT	0.499 ± .069	0.829 ± .023	0.599 ± .039	0.793 ± .015	0.266 ± .018	5.423 ± .904	6630.980 ± 268.285
SVM	0.629 ± .000	0.696 ± .000	0.905 ± .000	0.669 ± .000	0.202 ± .000	4.030 ± .000	7563.633 ± .000
SVM (RelAgg)	1.000 ± .000	0.922 ± .000	0.956 ± .019	0.777 ± .001	0.010 ± .000	1.612 ± .327	6354.633 ± 200.827
SVM (DT)	0.653 ± .174	0.916 ± .004	0.843 ± .086	0.763 ± .020	0.325 ± .014	2.429 ± .000	6128.120 ± 79.470
SVM (mRMR)	0.515 ± .005	0.922 ± .001	0.514 ± .023	0.312 ± .126	-	-	-
SVM (KW)	0.513 ± .006	0.922 ± .000	0.812 ± .078	0.780 ± .000	-	-	-

E-commerce I

	SCORE	False	True								
PageValues	0,79	0,90	0,70	0,00	0,00	3,46...	0,09	2,43	25,00		
ProductRelated	0,18	0,09	0,38	170,00	21,00	429,00...	69,00	117,00	22,00		
Administrative	0,13	0,07	0,24	5,00	0,00	19,00...	12,00	2,00	13,00		
TrafficType_14	0,09	0,04	0,17	0,00	0,00	0,00...	0,00	0,00	0,00		
TrafficType_9	0,08	0,05	0,15	0,00	0,00	0,00...	0,00	0,00	0,00		
ProductRelated_Duration	0,08	0,04	0,19	5.639,22	706,70	9.661,59...	2.269,73	4.185,10	1.525,00		
...
Browser_4	...	0,00	0,00	...	0,00	...	0,00	...	0,00	...	0,00

Table heatmap for e-commerce dataset.



E-commerce II

According to [Sakar et al., 2019]:

“Page Values”...

- is the most informative feature.

“Product Related”...

- is related to the class variable.
- was ranked in the lower positions.
- high correlation of this feature with the already selected “Page Values.”
- was not penalized by the neural network (due to redundancy).

It is clear from the relevance scores that “Page Values” is the major contributor to the network prediction.

ENEM 2016 I

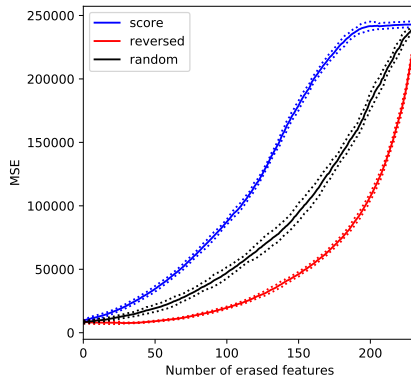
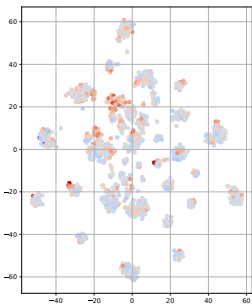


Figure: Perturbation analysis for neural networks trained on the ENEM dataset. Note that because the y-axis is the MSE, an increase in the values shows the deterioration of the predictions.

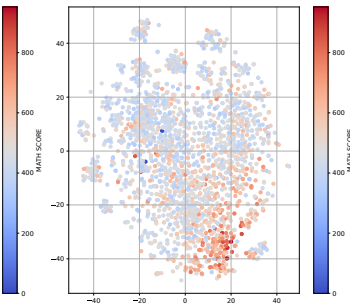
ENEM 2016 II

	SCORE	0.0 to 700	700 to 952	328.1	338.7	339.6	895.5	897.1	916.7
NATURAL SCIENCES	0,97	0,95	0,99	509,60	382,70	471,70	746,30	751,60	744,20
GENDER	0,66	0,70	0,62	1,00	1,00	1,00	0,00	0,00	0,00
Q020	0,65	0,70	0,61	1,00	1,00	1,00	1,00	0,00	0,00
Q025	0,63	0,66	0,60	1,00	0,00	0,00	1,00	1,00	1,00
Q021	0,58	0,67	0,50	0,00	0,00	0,00	0,00	1,00	0,00
Q042.H	0,01	...	0,02	...	0,01	...	0,00	...	0,00

Table heatmap for ENEM dataset.



Original.



Weighted.

ENEM 2016 III

“Natural Sciences”...

- is correlated in the dataset (0.584).
- “sanity check.”

“Gender”...

- machine bias.

Breast cancer gene expression I

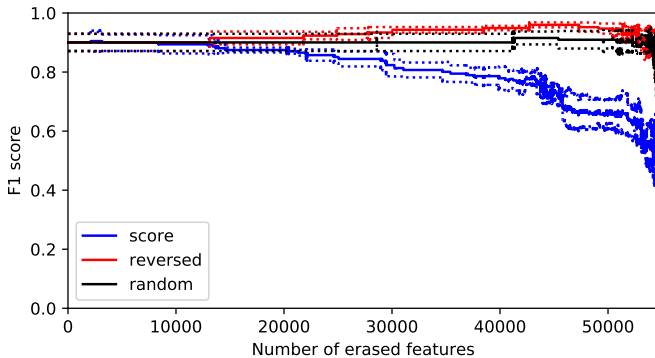


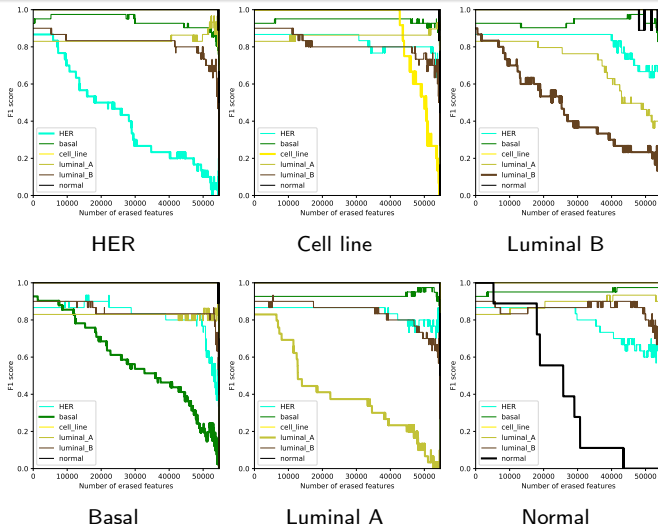
Figure: Perturbation analysis for neural networks trained on the breast cancer dataset.

Breast cancer gene expression II

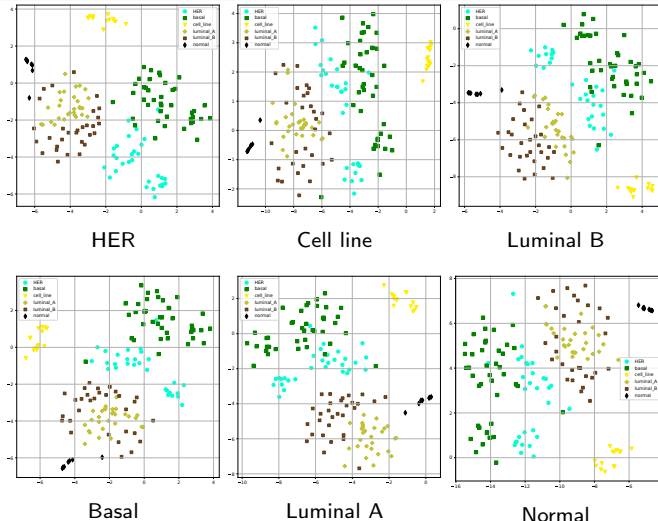
	SCORE	HER	Basal	Cell line	Luminal A	Luminal B	Normal
240701_at	0,416	0,636	0,585	0,501	0,297	0,477	0,196
223259_at	0,390	0,567	0,765	0,412	0,241	0,447	0,184
205635_at	0,389	0,512	0,327	0,371	0,360	0,280	0,556
206560_s_at	0,385	0,287	0,679	0,421	0,266	0,317	0,475
219415_at	0,383	0,256	0,773	0,380	0,270	0,291	0,534
...
217051_s_at	0,030	0,055	0,162	0,033	0,057	0,065	0,001

Figure: Excerpt of the table heatmaps for the breast cancer data.

Breast cancer gene expression III



Breast cancer gene expression IV



Outline

1 Introduction

2 Relevance Aggregation

3 Weighted t-SNE

4 Application to cancer data

5 Conclusion

Visualizing feature scoring I

- An inadequate set of scores can harm the subsequent chain of data analysis.
- Several distinct feature scorers, but no single metric or ground-truth able to guarantee the quality of the results.
- Visualization can become a valuable tool in informing the decision of which method to choose and how well are the results.
- The visualization of a low-dimensional embedding of the high-dimensional data is an established aspect of exploratory data analysis [Sohns et al., 2021].
- The possibility to visualize in a 2D scatterplot the clusters being affected by the feature importance scores would be a valuable tool to compare feature scorers.
- Few works are interested in displaying the effects of feature scoring.

Visualizing feature scoring II

How to visualize the outcome of different feature scorers?

- Account for non-linearity in the data;
- Be model-agnostic;
- Use the importance score of each feature to produce a corresponding embedding;
- Consider all features in the original dataset if all of them have an importance score larger than zero;
- Allow for comparisons.

Visualization methods

- ① PCA [Pearson, 1901]
- ② t-SNE [Maaten and Hinton, 2008]
- ③ SmartStripes [May et al., 2011]
- ④ UMAP [McInnes et al., 2018]
- ⑤ attribute-RadViz [Artur and Minghim, 2019]
- ⑥ FDive [Dennig et al., 2019]
- ⑦ Table heatmap [Grisci et al., 2021]

Current issues with feature scoring visualization: non-linearity, number of features, visualization of all features...

t-Distributed Stochastic Neighbor Embedding

- ① Non-linear dimensionality reduction technique.
- ② It preserves the local neighborhood of points.
- ③ The global structure of the dataset can be lost.
- ④ The low-dimensional embedding space does not necessarily represent any meaningful dimension of the original space.
- ⑤ Well established in large biological datasets.

t-SNE

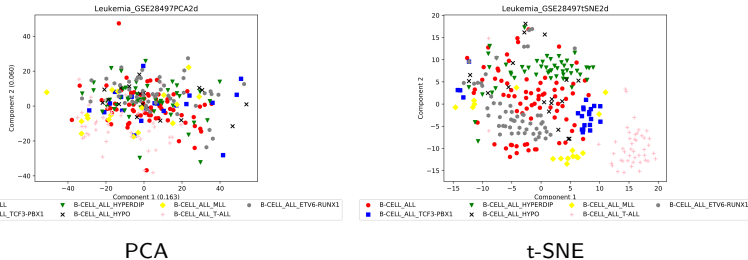


Figure: Comparison between the visualization using PCA and t-SNE of the Leukemia GSE28497 with 22284 genes. [Feltes et al., 2019]

Weighted t-SNE

$$d_w(\phi, \psi, \omega) = \sum_{i=1}^N \sqrt{(\omega_i(\psi_i - \phi_i))^2} \quad (3)$$

$$\omega_i(\psi_i - \phi_i) = (\psi_i \cdot \omega_i) - (\phi_i \cdot \omega_i) \quad (4)$$

[Horan, 1969, Carroll and Chang, 1970]

Silhouette coefficient

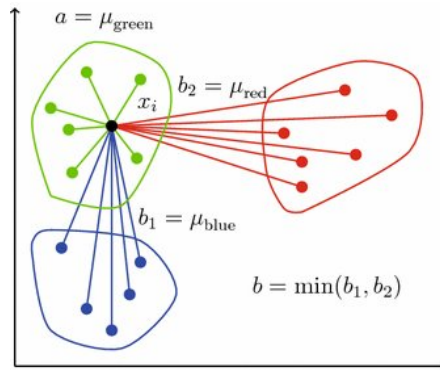


Figure: Example of silhouette coefficient.

[Narra et al., 2016]

Datasets

Table: Description of the datasets used in the weighted t-SNE experiments.
“Relevant” is the number of features which are relevant to the task. All datasets are numerical and tabular.

Dataset	Samples	Features	Relevant	Classes	Origin	Reference
XOR	500	50	2	2	Synthetic	[Tan et al., 2009, Grisci et al., 2021]
Synth	100	5000	50	2	Synthetic	[Guyon, 2003, Pedregosa et al., 2011]
Liver	48	22284	Unknown	2	Microarray	[Feltes et al., 2019]
Prostate	115	12647	Unknown	2	Microarray	[Feltes et al., 2019]
Regression	1000	100	4	-	Synthetic	[Celeux et al., 2012, Pedregosa et al., 2011]
Mouse cortex	23822	45769	Unknown	23	RNA-seq	[Tasic et al., 2018, Kobak and Berens, 2019]

Feature scorers

Table: Properties of the feature scorers used in the experiments. The type refers to how the scorer works and the correlation to how interactions between features are treated.

Scorer	Type	Correlation	Ref.
Kruskal-Wallis	Filter	Univariate	[Kruskal and Wallis, 1952]
Mutual Information	Filter	Univariate	[Vergara and Estévez, 2014]
mRMR	Filter	Multivariate	[Peng et al., 2005]
ReliefF	Filter	Multivariate	[Kononenko et al., 1997]
Lasso	Embedded	Multivariate	[Fonti and Belitser, 2017]
Decision Tree	Embedded	Multivariate	[Stone, 1984]
Random Forest	Ensemble	Multivariate	[Breiman, 2001]
Linear SVM	Embedded	Multivariate	[Cortes and Vapnik, 1995]
Neural Network	Embedded	Multivariate	[Grisci et al., 2021]

XOR

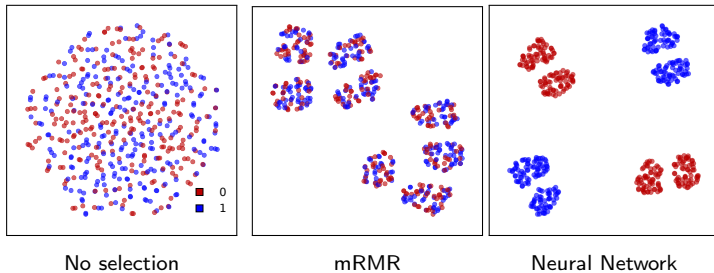


Figure: Visual comparison of feature scorers.

<https://sbcblab.github.io/wtsne/>

Synth

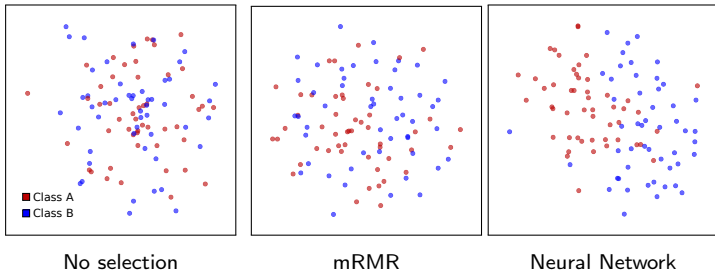


Figure: Visual comparison of feature scorers.

Liver cancer

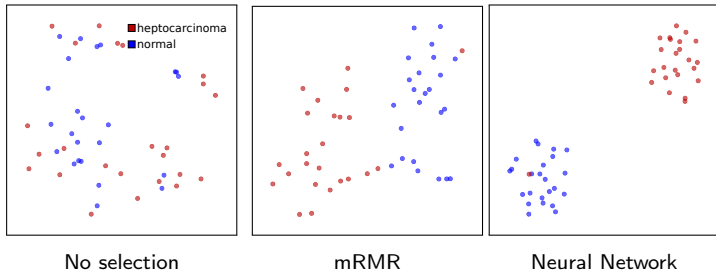


Figure: Visual comparison of feature scorers.

Prostate cancer

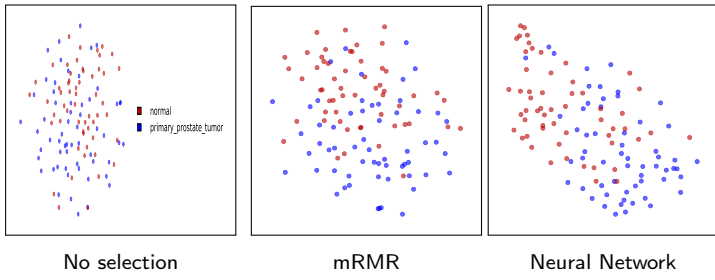


Figure: Visual comparison of feature scorers.

Mouse cortex

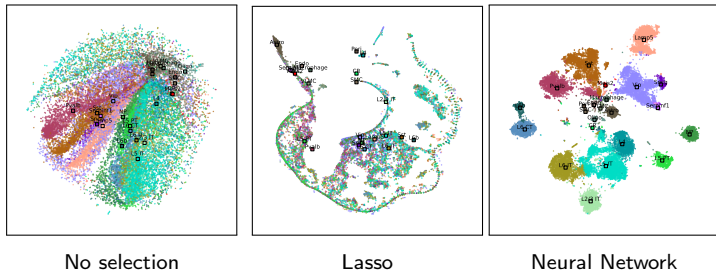
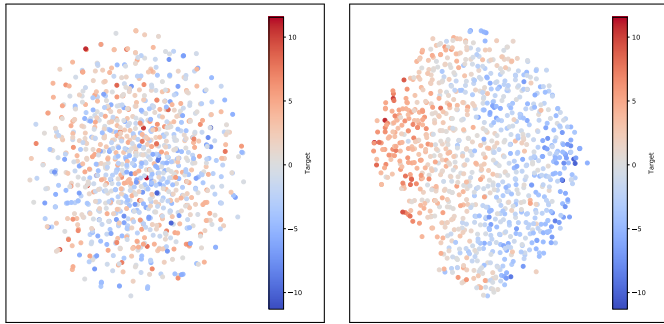


Figure: Visual comparison of feature scorers.

Regression



No feature importance

Feature importance as learned by a neural network

Figure: Comparison between the visualization using weighted t-SNE of a synthetic regression dataset before and after considering the feature importance as learned by a neural network.

Outlier detection

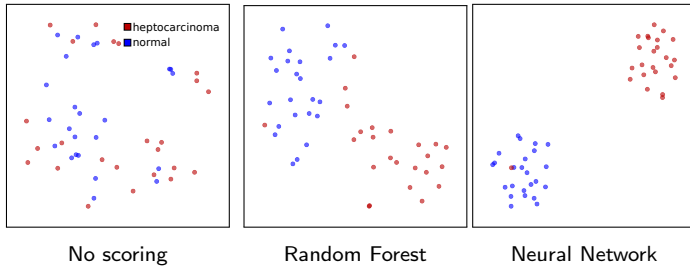
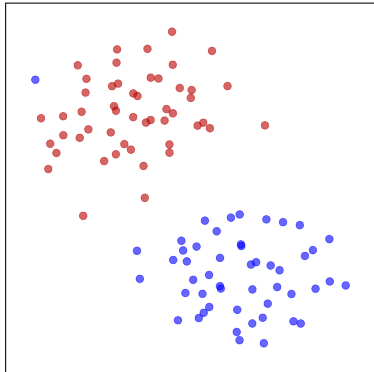


Figure: The sample that appears out of place has the accession code GSM557108: "liver tissue of subject 15, tumor"¹. The healthy samples are from the adjacent tissue of primary heptocarcinoma samples², so it is possible that this outlier was actually a healthy sample that was mislabeled, or perhaps a tumor sample with contamination from neighboring healthy tissue.

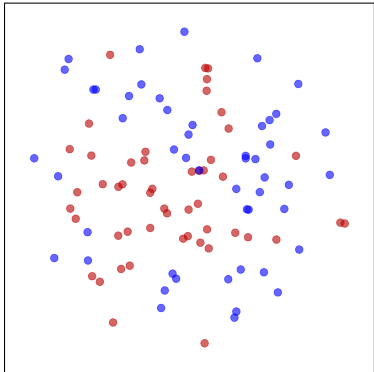
¹<https://www.ncbi.nlm.nih.gov/geo/query/acc.cgi?acc=GSM557108>

²<https://www.ncbi.nlm.nih.gov/geo/query/acc.cgi?acc=GSE22405>

“Perfect” selection



Kruskal-Wallis



“Perfect” selection

Figure: Comparison between the Kruskal-Wallis Filter and a “perfect” selection.

Evaluation I

Table: Silhouette coefficient, KL divergence, and F1-score of a kNN trained on the data for four distinct datasets and nine feature scorers.

	XOR				Synth				Liver				Prostate			
	HD	2D	KL	kNN	HD	2D	KL	kNN	HD	2D	KL	kNN	HD	2D	KL	kNN
No scoring	0.000	0.003	2.12	0.58	0.001	-0.009	0.16	0.63	0.038	0.038	0.14	0.68	0.008	0.046	0.51	0.58
Kruskall Wallis	0.004	0.010	0.48	0.51	0.041	0.609	0.56	1.00	0.183	0.449	0.15	0.94	0.072	0.196	0.35	0.71
Mutual Information	0.000	-0.001	1.19	0.54	0.006	0.180	0.69	0.66	0.133	0.234	0.15	0.94	0.025	0.121	0.49	0.68
mRMR	0.000	-0.002	0.74	0.54	0.008	0.030	0.77	0.56	0.228	0.560	0.18	0.94	0.031	0.156	0.54	0.66
ReliefF	0.104	0.204	0.80	1.00	0.005	0.433	0.33	0.97	0.128	0.333	0.18	0.94	0.018	0.126	0.48	0.68
Lasso	0.000	0.005	1.54	0.55	0.001	0.052	0.16	0.60	0.039	0.033	0.14	0.68	0.008	0.027	0.51	0.55
Decision Tree	-0.001	-0.002	0.65	0.58	0.050	0.058	0.48	0.61	0.358	0.422	0.07	0.81	0.078	0.122	0.42	0.71
Random Forest	0.089	0.204	0.91	1.00	0.014	0.045	0.74	0.67	0.235	0.490	0.21	0.94	0.052	0.162	0.51	0.73
Linear SVM	0.000	-0.001	1.59	0.56	0.002	0.180	0.19	0.64	0.040	0.037	0.16	0.81	0.008	0.049	0.55	0.60
Neural Network	0.148	0.192	0.49	1.00	0.014	0.200	0.65	0.85	0.387	0.782	0.17	0.94	0.098	0.200	0.40	0.73

Evaluation II

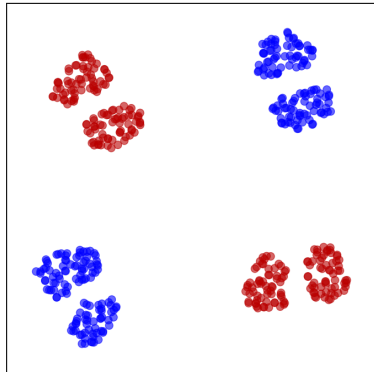
Table: Trustworthiness of the 2D t-SNE and weighted t-SNE projections for all datasets feature scorers.

	XOR	Synth	Liver	Prostate	Regression	Mouse cortex
No scoring	0.814	0.653	0.939	0.809	0.714	0.548
Kruskal-Wallis	0.997	0.863	0.949	0.896	-	-
Mutual Information	0.978	0.728	0.949	0.843	-	-
mRMR	0.990	0.792	0.937	0.821	-	-
ReliefF	0.978	0.701	0.954	0.826	-	-
Lasso	0.934	0.648	0.943	0.815	-	0.995
Decision Tree	0.987	0.921	0.984	0.930	-	-
Random Forest	0.974	0.806	0.937	0.871	-	0.998
Linear SVM	0.930	0.647	0.937	0.797	-	-
Neural Network	0.993	0.834	0.956	0.921	0.681	0.979

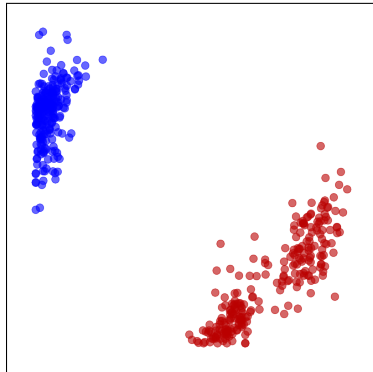
Machine Learning Interpretability

- Visualization of feature importance learned by DT, RF, Lasso, SVM, and NN.
- Weighted t-SNE can help interpretation by visually displaying the impact of the importance of the learned features.
- Regression: 4 truly relevant features out of 100, and the NN gave the largest importance scores to 3 of them (0.44, 0.40, 0.25, while the next largest score of 0.20 was given to an irrelevant feature and the fourth truly relevant feature received a score of 0.11).
- XOR: one can visually intuit that the NN and the RF learned a correct representation of the problem and that the DT and the linear SVM did not before even seeing the accuracy of these models.

Activation of the neurons



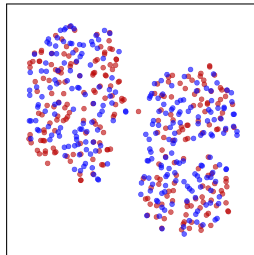
Weighted t-SNE



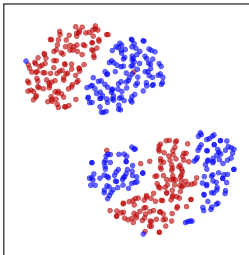
Activation of last layer neurons

Figure: Comparison between the weighted t-SNE and the activation of the neurons in the last layer of a neural network.

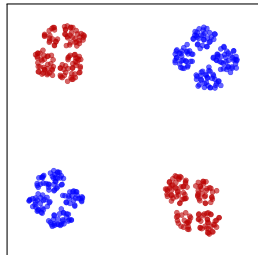
Evolution of learning



Epoch: 45
Loss: 0.844
SC: -0.0008



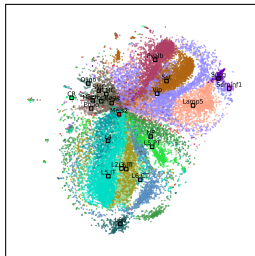
Epoch: 90
Loss: 0.726
SC: 0.0875



Epoch: 135
Loss: 0.366
SC: 0.1992

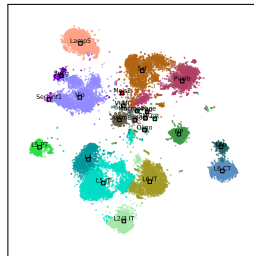
Figure: Visualization of the training of a neural network with the XOR dataset.

Evolution of learning II



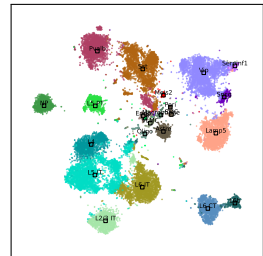
Epoch: 2

Loss: 19.65 | SC: -0.049



Epoch: 6

Loss: 4.56 | SC: 0.344



Epoch: 8

Loss: 3.86 | SC: 0.367

Figure: Visualization of the training of a neural network with the mouse cortex dataset.

Evolution of learning III

Table: Pearson correlation between training loss of neural network and the corresponding silhouette coefficient of the weighted t-SNE 2D embedding.

Dataset	Correlation
XOR	-0.85
Synth	-0.37
Liver	-0.81
Prostate	-0.67
Regression	-0.74
Mouse cortex	-0.98

Outline

1 Introduction

2 Relevance Aggregation

3 Weighted t-SNE

4 Application to cancer data

5 Conclusion

CuMiDa experiments

Table: Improvement of silhouette coefficient for all the CuMiDa datasets.

	F ₁ -score	SC Original	SC RelAgg	Increase factor
GSE31189	0.847	0.002	0.250	125.0
GSE50161	0.974	0.006	0.441	73.5
GSE22820	1.000	0.069	0.187	2.7
GSE26304	0.979	-0.300	-0.100	3.0
GSE42568	0.981	0.389	0.543	1.4
GSE45827	0.994	0.218	0.397	1.8
GSE59246	1.000	0.077	0.529	6.9
GSE70947	0.993	0.248	0.469	1.9
GSE21510	1.000	0.456	0.758	1.7
GSE41657	1.000	0.186	0.323	1.7
GSE44076	1.000	0.655	0.854	1.3
GSE44861	0.990	0.167	0.513	3.1
GSE28497	0.995	0.088	0.402	4.6
GSE63270	1.000	0.379	0.883	2.3
GSE14520 U133A	0.980	0.309	0.706	2.3
GSE62232	1.000	0.296	0.487	1.6
GSE76427	1.000	0.363	0.689	1.9
GSE18842	1.000	0.502	0.936	1.9
GSE19804	1.000	0.077	0.831	10.8
GSE6008	1.000	0.015	0.139	9.3
GSE6919 U95Av2	0.823	0.105	0.244	2.3
GSE6919 U95B	1.000	0.034	0.244	7.2
GSE6919 U95C	1.000	0.033	0.221	6.7
GSE53757	1.000	0.409	0.511	1.2
GSE42743	0.988	0.036	0.561	15.6
Average	0.982 ± 0.045	0.193 ± 0.208	0.481 ± 0.261	11.7 ± 27.6

CuMiDa experiments

Table: Details about the breast cancer and brain cancer datasets.

Type	Code	Submission year	Last update year	Platform
Breast	GSE22820	2010	2019	Agilent-014850 Whole Human Genome Microarray 4x44K G4112F
Breast	GSE26304	2010	2015	Agilent-012391 Whole Human Genome Oligo Microarray G4112A
Breast	GSE42568	2012	2019	Affymetrix Human Genome U133 Plus 2.0 Array
Breast	GSE45827	2013	2019	Affymetrix Human Genome U133 Plus 2.0 Array
Breast	GSE59246	2014	2018	Agilent-028004 SurePrint G3 Human GE 8x60K Microarray
Breast	GSE70947	2015	2018	Agilent-028004 SurePrint G3 Human GE 8x60K Microarray
Brain	GSE50161	2013	2019	Affymetrix Human Genome U133 Plus 2.0 Array

Breast cancer

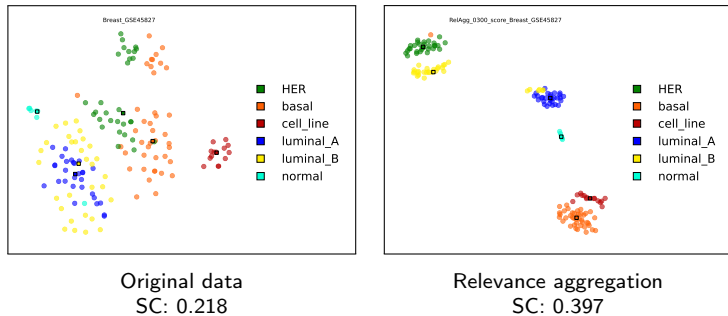
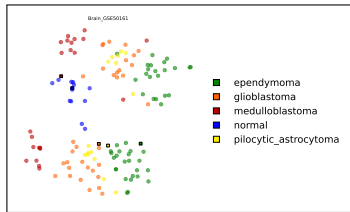
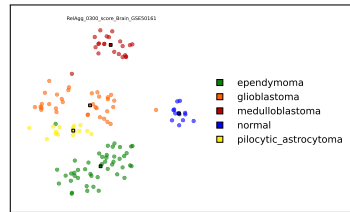


Figure: Breast GSE45827 F₁-score: 0.994

Brain cancer



Original data
SC: 0.006



Relevance aggregation
SC: 0.441

Figure: Brain GSE50161 F₁-score: 0.974

Feature selection

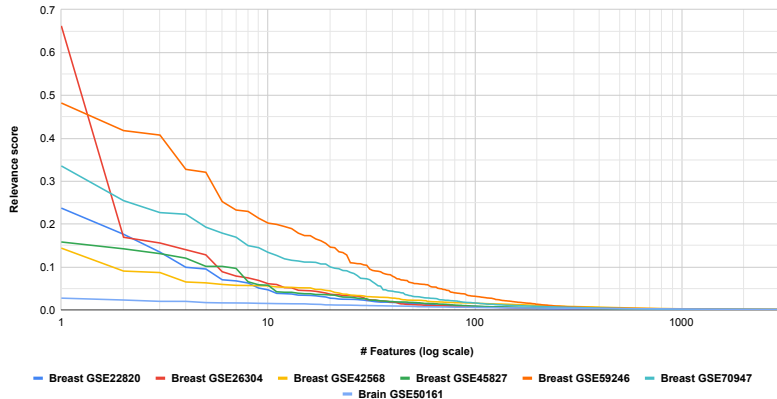


Figure: Relevance score of each feature of the seven cancer datasets.

Gene ontology: Breast cancer I



Figure: Gene ontology network for the six breast cancer datasets.

Gene ontology: Breast cancer II

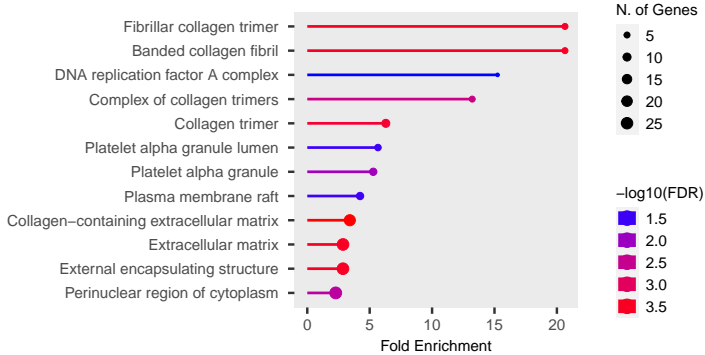


Figure: The major cellular components for genes in the six breast cancer datasets.

Gene ontology: Breast cancer III

Table: Gene ontology: disease

Enrichment FDR	nGenes	Pathway Genes	Fold Enrichment	Pathway
0.0268	3	12	16.52	DOID:13948 bladder neck obstruction
0.0026	5	20	16.52	DOID:13359 Ehlers-Danlos syndrome
0.0440	3	18	11.01	DOID:2378 relapsing-remitting multiple sclerosis
0.0469	3	19	10.43	DOID:90 degenerative disc disease
0.0232	5	40	8.26	DOID:0050848 obstructive sleep apnea
0.0440	4	36	7.34	DOID:12236 primary biliary cirrhosis
0.0066	7	65	7.12	DOID:10591 pre-eclampsia
0.0066	7	68	6.80	DOID:2349 arteriosclerosis
0.0469	4	39	6.78	DOID:4001 ovarian carcinoma
0.0440	5	61	5.42	DOID:11476 osteoporosis
0.0288	6	74	5.36	DOID:8398 osteoarthritis
0.0301	6	78	5.08	DOID:3770 pulmonary fibrosis
0.0484	5	66	5.01	DOID:5082 liver cirrhosis
0.0361	6	82	4.83	DOID:0050700 cardiomyopathy
0.0301	9	169	3.52	DOID:11054 urinary bladder cancer
0.0026	18	368	3.23	DOID:10763 hypertension
0.0288	12	269	2.95	DOID:5844 myocardial infarction
0.0301	12	279	2.84	DOID:1612 breast cancer

Gene ontology: Brain cancer I

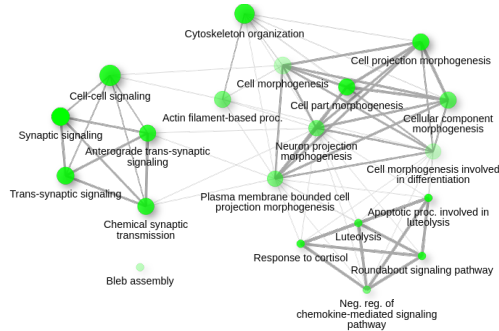


Figure: Gene ontology network for the brain cancer dataset.

Gene ontology: Brain cancer II

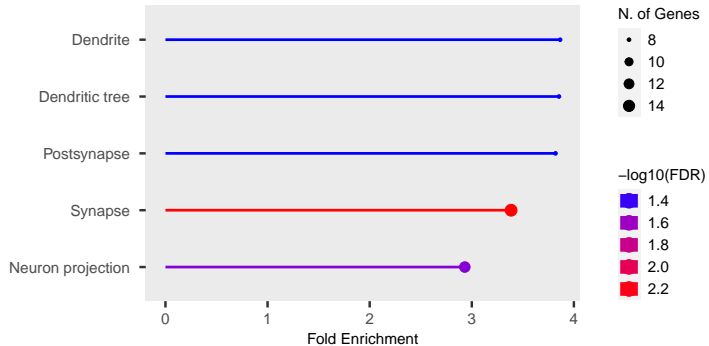


Figure: The major cellular components for genes in the brain cancer datasets.

Gene ontology: Brain cancer III

Table: Gene ontology: diseases

Enrichment FDR	nGenes	Pathway Genes	Fold Enrichment	Pathway
0.0643	2	21	31.01	DOID:6419 tetralogy of Fallot
0.0643	2	28	23.26	DOID:3827 congenital diaphragmatic hernia
0.0643	2	30	21.71	DOID:10908 hydrocephalus
0.0790	2	49	13.29	DOID:10754 otitis media
0.0880	2	60	10.86	DOID:1184 nephrotic syndrome
0.0643	3	92	10.62	DOID:3021 acute kidney failure
0.0643	4	139	9.37	DOID:2316 brain ischemia
0.0895	2	73	8.92	DOID:1596 mental depression

Review of genes

Table: Number of publications in PubMed relating the selected genes to cancer (last 5 years).

	PubMed		PubMed	
	Breast cancer	Any cancer	Brain cancer	Any cancer
<i>HS3ST4</i>	1	1	<i>MNX1-AS1</i>	5
<i>COL1A1</i>	56	530	<i>OBP2B</i>	0
<i>MUC4</i>	19	225	<i>LOXL4</i>	1
<i>STARD3</i>	8	19	<i>OBP2A</i>	0
<i>CR1</i>	6	368	<i>MYO3A</i>	0
<i>THY1</i>	13	119	<i>WNT4</i>	3
<i>LRRK3B</i>	2	6	<i>HBG1</i>	0
<i>MUCL1</i>	5	6	<i>LSP1</i>	4
<i>PGA3</i>	1	3	<i>TNN</i>	3
<i>ERBB2</i>	5918	8043	<i>GTF2H2</i>	0
<i>PCDHA6</i>	0	0	<i>HMGB3</i>	5
<i>GLYAT</i>	2	3	<i>RBM3</i>	3
<i>CTHRC1</i>	9	88	<i>CREB5</i>	1
<i>GATA3</i>	373	983	<i>ARHGEF33</i>	0
<i>CA12</i>	13	51	<i>LPAR3</i>	1
<i>ANXA9</i>	2	7	<i>SLIT2</i>	8
<i>STARD10</i>	2	3	<i>PTN</i>	11
<i>PRKD3</i>	5	17	<i>PAX1</i>	1
<i>PPARA</i>	10	112	<i>SALL3</i>	2
				15

Outline

1 Introduction

2 Relevance Aggregation

3 Weighted t-SNE

4 Application to cancer data

5 Conclusion

Contributions I

Improving the interpretability of deep learning on tabular data

- Development of the relevance aggregation method to understand neural networks applied to tabular data, a type of data that is often overlooked in research.
- Demonstration of the effectiveness of relevance aggregation for feature selection in various types of tabular data.
- Demonstration that the neural networks are indeed using the features identified as relevant by relevance aggregation.
- Proposal of visualization methods (table heatmaps and weighted t-SNE) to analyze and interpret the results of relevance aggregation.
- The use of weighted t-SNE and silhouette coefficient to visualize and compare machine learning and feature scorer algorithms.

Contributions II

Acquisition of relevant biological knowledge from artificial neural networks

- Study of the extraction of relevant biological information from gene expression data using neural networks through relevance aggregation and weighted t-SNE.
- Identification of genes with higher relevance scores obtained from neural networks linked to known cancer bioprocesses and cellular components.
- This identification happens automatically without explicit instructions.
- Validation of the findings through functional enrichment analysis and literature review of the connections between the genes and cancers.

References I

-  [Artur, E. and Minghim, R. \(2019\).](#)
A novel visual approach for enhanced attribute analysis and selection.
Computers & Graphics, 84:160–172.
-  [Bach, S., Binder, A., Montavon, G., Klauschen, F., Müller, K.-R., and Samek, W. \(2015\).](#)
On pixel-wise explanations for non-linear classifier decisions by layer-wise relevance propagation.
Plos One, 10(7):e0130140.

References II

-  Binder, A., Bockmayr, M., Hägele, M., Wienert, S., Heim, D., Hellweg, K., Stenzinger, A., Parlow, L., Budczies, J., Goeppert, B., et al. (2018).
Towards computational fluorescence microscopy: machine learning-based integrated prediction of morphological and molecular tumor profiles.
arXiv preprint arXiv:1805.11178.
-  Böhle, M., Eitel, F., Weygandt, M., and Ritter, K. (2019).
Layer-wise relevance propagation for explaining deep neural network decisions in mri-based alzheimer's disease classification.
Frontiers in Aging Neuroscience, 11:194.
-  Breiman, L. (2001).
Random forests.
Machine Learning, 45(1):5–32.

References III

-  Carroll, J. D. and Chang, J.-J. (1970).
Analysis of individual differences in multidimensional scaling via an n-way generalization of “eckart-young” decomposition.
Psychometrika, 35(3):283–319.
-  Celeux, G., El Anbari, M., Marin, J.-M., Robert, C. P., et al. (2012).
Regularization in regression: comparing bayesian and frequentist methods in a poorly informative situation.
Bayesian Analysis, 7(2):477–502.
-  Cortes, C. and Vapnik, V. (1995).
Support-vector networks.
Machine Learning, 20(3):273–297.

References IV

-  Dennig, F. L., Polk, T., Lin, Z., Schreck, T., Pfister, H., and Behrisch, M. (2019).
Fdive: Learning relevance models using pattern-based similarity measures.
In *2019 IEEE Conference on Visual Analytics Science and Technology (VAST)*, pages 69–80, Vancouver, BC, Canada. IEEE.
-  Feltes, B. C., Chandelier, E. B., Grisci, B. I., and Dorn, M. (2019).
Cumida: An extensively curated microarray database for benchmarking and testing of machine learning approaches in cancer research.
Journal of Computational Biology, 26(4):376–386.
-  Fonti, V. and Belitser, E. (2017).
Feature selection using lasso.
VU Amsterdam Research Paper in Business Analytics, 30:1–25.

References V

-  Grisci, B. I., Krause, M. J., and Dorn, M. (2021).
Relevance aggregation for neural networks interpretability and knowledge discovery on tabular data.
Information Sciences, 559:111–129.
-  Guyon, I. (2003).
Design of experiments of the nips 2003 variable selection benchmark.
In *NIPS 2003 Workshop on Feature Extraction and Feature Selection*, volume 253, pages 1–30, Whistler. NIPS.
-  Horan, C. B. (1969).
Multidimensional scaling: Combining observations when individuals have different perceptual structures.
Psychometrika, 34(2):139–165.

References VI

-  Kobak, D. and Berens, P. (2019).
The art of using t-sne for single-cell transcriptomics.
Nature Communications, 10(1):1–14.
-  Kononenko, I., Šimec, E., and Robnik-Šikonja, M. (1997).
Overcoming the myopia of inductive learning algorithms with relieff.
Applied Intelligence, 7(1):39–55.
-  Kruskal, W. H. and Wallis, W. A. (1952).
Use of ranks in one-criterion variance analysis.
Journal of the American Statistical Association, 47(260):583–621.
-  Maaten, L. v. d. and Hinton, G. (2008).
Visualizing data using t-sne.
Journal of Machine Learning Research, 9(Nov):2579–2605.

References VII

-  May, T., Bannach, A., Davey, J., Ruppert, T., and Kohlhammer, J. (2011).
Guiding feature subset selection with an interactive visualization.
In *2011 IEEE Conference on Visual Analytics Science and Technology (VAST)*, pages 111–120, Providence, Rhode Island, USA. IEEE.
-  McInnes, L., Healy, J., and Melville, J. (2018).
Umap: Uniform manifold approximation and projection for dimension reduction.
arXiv preprint arXiv:1802.03426.
-  Montavon, G., Samek, W., and Müller, K.-R. (2018).
Methods for interpreting and understanding deep neural networks.
Digital Signal Processing, 73:1–15.

References VIII

-  **Narra, U., Troia, F. D., Corrado, V. A., Austin, T. H., and Stamp, M. (2016).**
Clustering versus svm for malware detection.
Journal of Computer Virology and Hacking Techniques, 12:213–224.
-  **Pearson, K. (1901).**
On lines and planes of closest fit to systems of points in space.
The London, Edinburgh, and Dublin Philosophical Magazine and Journal of Science, 2(11):559–572.
-  **Pedregosa, F., Varoquaux, G., Duchesnay, E., et al. (2011).**
Scikit-learn: Machine learning in Python.
Journal of Machine Learning Research, 12:2825–2830.

References IX

-  Peng, H., Long, F., and Ding, C. (2005). Feature selection based on mutual information criteria of max-dependency, max-relevance, and min-redundancy. *IEEE Transactions on Pattern Analysis and Machine Intelligence*, 27(8):1226–1238.
-  Sakar, C. O., Polat, S. O., Katircioglu, M., and Kastro, Y. (2019). Real-time prediction of online shoppers' purchasing intention using multilayer perceptron and lstm recurrent neural networks. *Neural Computing and Applications*, 31(10):6893–6908.

References X

-  Sohns, J.-T., Schmitt, M., Jirasek, F., Hasse, H., and Leitte, H. (2021). Attribute-based explanation of non-linear embeddings of high-dimensional data. *IEEE Transactions on Visualization and Computer Graphics*, 28(1):540–550.
-  Stone, C. J. (1984). *Classification and Regression Trees*. Taylor & Francis Group, LLC, Boca Raton, FL, 1st edition.
-  Tan, M., Hartley, M., Bister, M., and Deklerck, R. (2009). Automated feature selection in neuroevolution. *Evolutionary Intelligence*, 1(4):271–292.

References XI

-  Tasic, B., Yao, Z., Graybuck, L. T., Smith, K. A., Nguyen, T. N., Bertagnolli, D., Goldy, J., Garren, E., Economo, M. N., Viswanathan, S., et al. (2018). Shared and distinct transcriptomic cell types across neocortical areas. *Nature*, 563(7729):72–78.
-  Vergara, J. R. and Estévez, P. A. (2014). A review of feature selection methods based on mutual information. *Neural Computing and Applications*, 24(1):175–186.
-  Yang, Y., Tresp, V., Wunderle, M., and Fasching, P. A. (2018). Explaining therapy predictions with layer-wise relevance propagation in neural networks. In *2018 IEEE International Conference on Healthcare Informatics (ICHI)*, pages 152–162, New York, NY, USA. IEEE.